Population inversion and negative dynamic conductivity in optically pumped graphene

A. Satou*, F. T. Vasko†, T. Otsuji‡ and V. Ryzhii*
* Computational Nanoelectronics Laboratory, University of Aizu, Aizu-Wakamatsu 965-9580, Japan
† Institute of Semiconductor Physics, NAS of Ukraine, Kiev 03028, Ukraine
‡Research Institute of Electrical Communication, Tohoku University, Sendai 980-8577, Japan
e-mail: a-satou@u-aizu.ac.jp

***Abstract*—We study nonequilibrium carriers (electrons and holes) in an intrinsic graphene at low temperatures under infrared optical pumping. We calculate the energy distributions of carriers using a quasi-classical kinetic equation. It is found that the nonequilibrium distributions are determined by an interplay between weak energy relaxation on acoustic phonons and generation-recombination processes as well as by the effect of pumping saturation. We show that at certain pumping power density the population inversion as well as the dynamic negative conductivity can take place in terahertz and far-infrared frequencies, suggesting the possibility of utilization of graphene under optical pumping for optoelectronic applications, in particular, lasing at such frequencies.**

I. Introduction

The features of the dynamics of electrons and holes in graphene result in the exceptional properties of graphene. The studies of optical phenomena in graphene can be utilized for revealing the mechanisms of carrier scattering [1], [2]. The gapless energy spectrum of graphene provides its nontrivial optical properties which can be utilized in novel optoelectronic devices [3]–[5].

Due to zero band gap, the carrier distributions near the Dirac point in intrinsic graphene can exceed one half by even weak optical pumping, corresponding to population inversion. Previously we demonstrated that under the assumption that the distributions become quasi-equilibrium due to carrier-carrier collisions, population inversion and negative dynamic conductivity in the terahertz/far-infrared range are possible [3]. At low temperatures and not too strong pumping where carrier-carrier collisions can be ineffective, however, the carrier distributions are determined by an interplay between acoustic phonon scattering and thermal generation/recombination processes [6].

In this paper, we study nonequilibrium carriers (electrons and holes) in an intrinsic graphene at low temperatures under near-infrared optical pumping following the cascade of optical phonons. We calculate the energy distributions of carriers using a quasi-classical kinetic equation which accounts for the energy relaxation due to acoustic phonons and the radiative generation-recombination processes associated with thermal radiation, the the cascade emission of optical phonons, and the carrier photoexcitation by incident radiation. It is found that the nonequilibrium distributions are determined by an interplay between weak energy relaxation on acoustic phonons and generation-recombination processes as well as by the effect of pumping saturation. The steady-state and dynamic conductivities are calculated as well. It is shown that the population inversion and negative dynamic conductivity can take place at rather wide ranges of terahertz and far-infrared frequencies. These facts suggest that graphene under optical pumping can be utilized for optoelectronic applications, in particular, for the terahertz and/or far-infrared lasers.

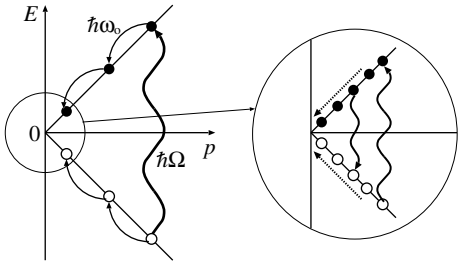

Fig. 1. Schematic view of graphene band structure. The arrows show different interband and intraband transitions: absorption of photons with energy $\hbar\Omega$, emission of optical phonons with energy $\hbar\omega_o$, thermal photon generation/recombination, and carrier energy relaxation by quasi-elastic acoustic phonons.

II. Model

The model accounts for the absorption of pumping photons with energy $\hbar\Omega$, cascade emission of optical phonons with energy $\hbar\omega_o \simeq 198$ meV, thermal photon generation/recombination processes, and quasi-elastic acoustic phonon scattering (see Fig. 1). In contrast to [6], where the pumping which does not involve any optical phonon emission (direct pumping) was studied, the pumping which results in emission of optical phonons is considered here. We assume that the pumping photon energy is close to the even multiple of the optical phonon energy, so that the cascade emission of optical phonons results in the accumulation of carriers near the Dirac point. The steady-state kinetic equation for the carrier distribution function f_p is given by [6]

$$J_{LA}\{f_p\} + J_R\{f_p\} + G\{f_p\} = 0, \qquad (1)$$

where $J_{LA}\{f_p\}$ and $J_R\{f_p\}$ are the collision integrals associated with the relaxation of carriers caused by the acoustic phonon scattering and the thermal photon generation/recombination processes, respectively, and $G\{f_p\}$ de-

978-1-4244-3947-8/09/$25.00 ©2009 IEEE

scribes the generation of electron-hole pair due to the optical excitation and the cascade emission of optical phonons. These are given by the following:

$$J_{LA}\{f_p\} = \frac{\gamma}{p^2}\frac{d}{dp}\left\{p^4\left[\frac{df_p}{dp} + \frac{f_p(1-f_p)}{p_T}\right]\right\}, \quad (2)$$

$$J_R\{f_p\} = \left[\frac{1-2f_p}{\exp(2p/p_T)-1} - f_p^2\right], \quad (3)$$

$$G\{f_p\} = (1-2f_p)\frac{S}{\overline{S}}\cdot\Delta\left(\frac{2v_{\rm W}p - \hbar\Omega^{(\rm eff)}}{\hbar\delta\Omega}\right), \quad (4)$$

where $\gamma = v_{\rm qe}/v_{\rm R}$ is the ratio of rates of acoustic phonon scattering and generation/recombination processes, $v_{\rm qe}$ and $v_{\rm R}$ are their characteristic velocities [9], respectively, $p_T = k_{\rm B}T/v_{\rm W}$, S is the pumping power density, $\overline{S}$ is the characteristic power density, $\Delta(z) = \exp(-z^2)/\sqrt{\pi}$ is a function representing the broadening of interband transitions, $\hbar\Omega^{(\rm eff)} = \hbar\Omega - 2N\hbar\omega_{\rm o}$, and $\hbar\delta\Omega \propto \hbar\Omega$ is the broadening energy of the absorbed photons. The characteristic power density $\overline{S}$ is given by

$$\overline{S} = \frac{k_{\rm B}Tv_{\rm R}c\sqrt{\varepsilon}(\hbar\Omega)^3}{2\pi^2e^2v_{\rm W}^3\hbar^2}\left(\frac{\delta\Omega}{\Omega}\right), \quad (5)$$

where e is the electron charge, c is the speed of light, and ε is the dielectric constant. Equation (1) is accompanied by the following boundary conditions [6]:

$$f_p\Big|_{p=0} = \frac{1}{2}, \qquad p^4\left[\frac{df_p}{dp} + \frac{f_p(1-f_p)}{p_T}\right]\Big|_{p\to\infty} = 0. \quad (6)$$

The numerical procedure for solving Eq. (1) was the following. First, we linearized Eq. (1) by setting $f_p = f^{(n)}$ and $f_p^2 = f^{(n-1)}f^{(n)}$ ($n = 1, 2, 3, \cdots$), solved the resultant ordinary differential equation for $f^{(n)}$ by the finite difference method, and continued the iteration for n until the convergence of $f^{(n)}$. Since the solution for $S = 0$ can be analytically found as $f_p(S=0) = [\exp(p/p_T)+1]^{-1}$, we started the procedure from small nonzero $S = S_1$, set the initial guess $f^{(0)} = f_p(S=0)$, invoked the iteration method, and found the approximate solution $f_p(S = S_1)$. Then we put $f^{(0)} = f_p(S = S_1)$ for larger S, and so on.

III. Results and discussion

Figure 2 shows the carrier distribution in graphene under the pumping at $T = 77$ K with $\hbar\Omega = 794$, 806, and 830 meV (corresponding to $\hbar\Omega^{(\rm eff)} = 2$, 14, and 38 meV). It was assumed that $v_{\rm R} = 41.6$ cm/s, $v_{\rm qe} = 0.72$ and 13.17 cm/s, $\delta\Omega/\Omega = 0.1$, and $\epsilon = 3.7$.

It can be clearly seen from Fig. 2 that above a certain pumping power density the distribution function can exceed 1/2, i.e., the population inversion can take place. It is shown that it takes place at nonzero carrier energy. This is because vanishing quasi-elastic relaxation near the Dirac point forces the carrier distribution function to be equilibrium. At strong pumping with very small pumping photon energy, however, photoexcited electrons and holes relaxed by optical phonon emission are directly accumulated at low energy region and the distribution function becomes almost 1/2 (see the bottom panel of Fig. 2). One can also see from the top and bottom panels of Fig. 2) that the lower power density is necessary for the population inversion at lower pumping photon energy. Comparing to the results of the pumping without any emission of optical phonon [6], the population inversion takes place at lower power density, although the maximum value of the distribution function is smaller.

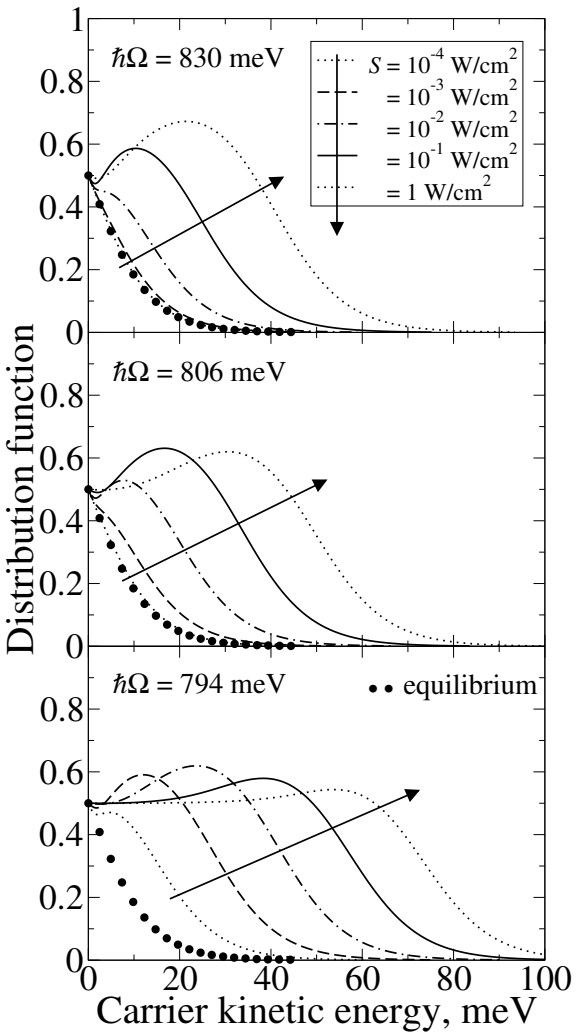

Fig. 2. Distribution vs carrier kinetic energy at $T = 77$ K for different pumping photon energies and different pumping power densities. Circles correspond to the equilibrium distributions.

The population inversion can lead to the negative dynamic conductivity at some signal frequency. The real part of the dynamic conductivity is given by [7]

$$\mathrm{Re}\,\sigma_\omega = \mathrm{Re}\,\sigma_\omega^{(\rm inter)} + \mathrm{Re}\,\sigma_\omega^{(\rm intra)}, \quad (7)$$

where $\sigma_\omega^{(\rm inter)}$ and $\sigma_\omega^{(\rm intra)}$ are the interband and intraband (Drude-like) contributions given by

$$\mathrm{Re}\,\sigma_\omega^{(\rm inter)} = \frac{e^2v_{\rm W}^2}{\hbar^3\omega\delta\omega}\int_0^\infty dpp(1-2f_p)\Delta\left(\frac{2v_{\rm W}p - \hbar\omega}{\hbar\delta\omega}\right), \quad (8)$$

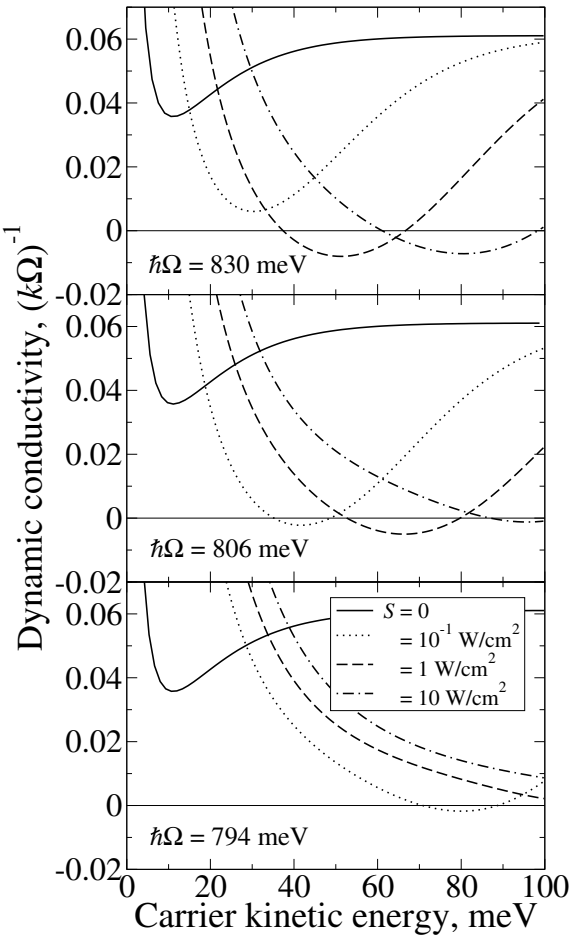

Fig. 3. Dynamic conductivity vs signal photon energy at $T = 77$ K for different pumping photon energies and different pumping power densities.

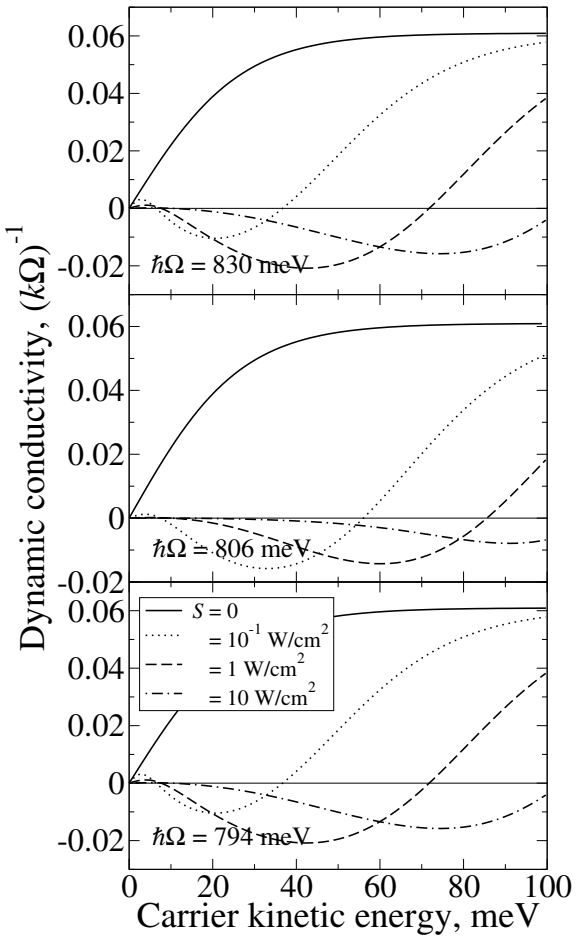

Fig. 4. Interband contribution of dynamic conductivity $\mathrm{Re}\,\sigma_\omega^{(\mathrm{inter})}$ vs signal photon energy at $T = 77$ K for different pumping photon energies and different pumping power densities.

$$\mathrm{Re}\,\sigma_\omega^{(\mathrm{intra})} = \frac{2e^2 v_{\mathrm{W}}}{\pi\hbar^2}\int_0^\infty dpp\left(-\frac{df_p}{dp}\right)\frac{\tau_p^{(\mathrm{m})}}{1+(\omega\tau_p^{(\mathrm{m})})^2}, \quad (9)$$

where $\tau_p^{(\mathrm{m})}$ is the momentum relaxation time associated with the disorder scattering [8]. Here we set the disorder scattering correlation length $l_c = 30$ nm. Since the integrand in the first term in Eq. (7) can be negative due to the population inverstion, the dynamic conductivity can be nagative as well. Figure 3 shows the dynamic conductivity as a function of the signal photon energy $\hbar\omega$. As seen in Fig. 3, the negative dynamic conductivity takes place at $\hbar\omega = 40 - 100$ meV ($f = 10 - 24$ THz), corresponding to terahertz/far-infrared frequencies. As the distribution function, the dynamic conductivity becomes negative at lower pumping power for smaller pumping photon energy. However, its absolute value is larger for larger pumping photon energy. Figure 4 shows the interband contribution of dynamic conductivity $\mathrm{Re}\,\sigma_\omega^{(\mathrm{inter})}$ as a function of the signal photon energy $\hbar\omega$. By comparing Fig. 4 to 3, one can see that, inspite of the fact that the interband contribution (8) exhibits large negative value, the intraband contribution (9) severely reduces the absolute value of the negative dynamic conductivity, especially in the case of smaller pumping photon energy.

IV. Conclusions

In conclusion, we calculated the energy distributions of carriers in an intrinsic graphene under the cascade pumping by near-infrared irradiation. We developed the model based on the quasi-classical kinetic equation which accounts for the energy relaxation due to acoustic phonons and the radiative generation-recombination processes associated with thermal radiation, the the cascade emission of optical phonons, and the carrier photoexcitation by incident radiation. We demonstrated that the carrier distribution function becomes nonequilibrium due to the interplay between acoustic phonon scattering and neration-recombination processes, and that it can exceed 1/2, i.e., the population inversion can take place. We also showed that the negative dynamic conductivity can take place at rather wide ranges of terahertz and far-infrared frequencies.

Acknowledgment

This work is partially supported by the Japan Science and Technology Agency, CREST, Japan.

REFERENCES

[1] S. Butscher, F. Milde, M. Hirtschulz, E. Malic, and A. Knorr, Appl. Phys. Lett. **91**, 203103 (2007).
[2] J. M. Dawlaty, *et al.*, Appl. Phys. Lett. **93**, 131905 (2008).
[3] V. Ryzhii, M. Ryzhii, and T. Otsuji, J. Appl. Phys. **101**, 083114 (2007).
[4] F. Rana, IEEE Trans. Nanotechnology **7**, 91 (2008).
[5] V. Ryzhii, V. Mitin, M. Ryzhii, N. Ryabova, and T. Otsuji, Appl. Phys. Express **1**, No. 6 (2008).
[6] A. Satou, F. T. Vasko, and V. Ryzhii, Phys. Rev. B **78**, 115431 (2008).
[7] L. A. Falkovsky and A. A. Varlamov, Eur. Phys. J. **56**, 281 (2007).
[8] F.T. Vasko and V. Ryzhii, Phys. Rev. B **77**, 195433 (2008).
[9] F.T. Vasko and V. Ryzhii, Phys. Rev. B **76**, 233404 (2007).